External Grant Award Number 03HQGR0082

EVOLUTION OF STRESS ALONG THE SOUTHERN SAN ANDREAS FAULT SYSTEM FOR THE PAST TWO CENTURIES

Andrew M. Freed and Tabrez Ali
Department of Earth and Atmospheric Sciences, Purdue University, 550 Stadium Mall Dr., West Lafayette, IN, 47906. *E-mail: freed@purdue.edu*

Roland Bürgmann
Department of Earth and Planetary Sciences, 389 McCone Hall, University of California, Berkeley, Berkeley, California, 94720

External Grant Award Number 03HQGR0082

EVOLUTION OF STRESS ALONG THE SOUTHERN SAN ANDREAS FAULT SYSTEM FOR THE PAST TWO CENTURIES

Andrew M. Freed and Tabrez Ali
Department of Earth and Atmospheric Sciences, Purdue University, 550 Stadium Mall Dr., West Lafayette, IN, 47906. *E-mail: freed@purdue.edu*

Roland Bürgmann
Department of Earth and Planetary Sciences, 389 McCone Hall, University of California, Berkeley, Berkeley, California, 94720

Abstract

The seismicity of southern California results from stresses that arise from the relative motion of the Pacific and North American Plates being accommodated along the San Andreas Fault (SAF) system and the Eastern California Shear zone (ECSZ). Here we calculate how the stress field in southern California has evolved over these past two centuries due to interseismic loading, as inferred from current GPS observations of surface velocities, from redistributions of static stress induced by large ($M_w \geq 6.5$) earthquakes since the 1812 Wrightwood quake, and postseismic viscoelastic relaxation associated with these events that serves to transfer coseismic stresses from the deep, warm, lower crust and upper mantle to the overlying seismogenic upper crust. We calculate Coulomb stress changes on vertical strike-slip faults striking parallel to the SAF and at the hypocenters on the rupture planes of all $M_w \geq 6$ events over the past two centuries. Our results suggest that the 1857 $M_w = 8.2$ Fort Tejon earthquake, by far the largest event to have occurred in the region over the past two centuries, had a profound influence on the state of stress in Southern California during the 19th century, inducing significant stress increases to the north (Parkfield region and adjoining creeping SAF) and south (southern SAF and San Jacinto fault), and stress relief across the southern ECSZ. These stress changes were then greatly magnified by postseismic relaxation through the early part of the 20th century. Slow interseismic build-up of stress further loads all major strike-slip faults and works to reload the areas of the ECSZ where stress was relieved by the 1857 quake. Our calculations suggest that only 56% of hypocenters were pushed closer to failure by preceding coseismic stress changes, suggesting that the occurrence of large earthquakes is not strongly determined by coseismic Coulomb stress changes. This percentage rises to 70% when postseismic stress changes are also considered. Our calculations demonstrate the importance of postseismic viscoelastic relaxation in the redistribution of stress following large earthquakes. We find, however, that postseismic processes associated with events more than about a decade old are near completion and thus do not significantly influence the regional velocity field presently observed in southern California.

1.0 Introduction

Having experienced more than 73 $M_w \geq 6$ earthquakes since 1812 (Kagan et al., 2006) (Figure 1), southern California is one of the most seismically active regions in the

conterminous United States. This high seismicity rate is a product of ~50 mm/yr of relative motion between the North American and Pacific plates (DeMets and Dixon, 1999), accommodated primarily by right-lateral slip on the SAF, other sub-parallel faults and the ECSZ. The southern SAF is capable of producing major ($M_w > 7.5$) earthquakes, two of which have occurred in the past two hundred years; at Wrightwood in 1812 (M_w = 7.5) and Fort Tejon in 1857 (M_w = 8.2) (Jacoby et al., 1988; Sieh et al., 1989); and the recent 1992 M_w = 7.3 Landers and 1999 M_w = 7.1 Hector Mine earthquakes showed that the EZCS is also capable of producing large events. In addition, the bend in the SAF in southern California has led to a zone of compression forming the Transverse Ranges and thrust earthquakes in the Los Angeles region, such as the 1994 M_w = 6.7 Northridge earthquake.

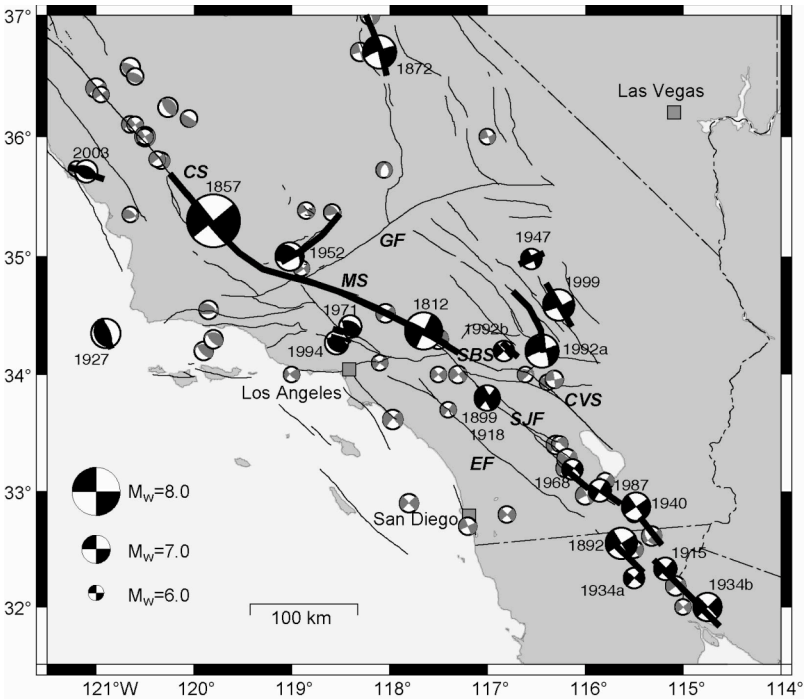

Figure 1. Earthquakes in southern California between 1812 and 2005 considered in this analysis. Black and white focal mechanisms show 21 earthquakes of $M_w \geq 6.5$ that are used to determine how coseismic slip and associated postseismic relaxation has influenced the southern California stress field since 1812 (Table 1). Grey and white focal mechanisms show 52 $6.0 \leq M_w < 6.5$ events where stress changes are determined for each hypocenter prior to rupture, but stress changes due to these ruptures are not considered in subsequent stress changes. Earthquake dates are only shown for $M_w \geq 6.5$ events. Thick lines show approximate rupture surface trace (or projected surface trace for blind thrusts) associated with each $M_w \geq 6.5$ event. Segments of the San Andreas Fault: CS – Cholame segment, MS – Mojave segment, SBS – San Bernardino Mountain segment, CVS – Coachella Valley segment; SJF – San Jacinto Fault; EF – Elsinore Fault.

Numerous studies have sought to understand the distribution of large earthquakes in space and time in southern California with the hope of improving forecasting and mitigation. Many of these efforts have concentrated on calculating the evolution of crustal stresses as a means to understanding patterns of earthquake occurrence. In a process referred to as fault interaction, earthquakes have been theorized to encourage or retard subsequent earthquakes in a region (see reviews by Stein, 1999, 2003; Harris, 1998; King and Cocco, 2001; Freed, 2005). In some regions large earthquakes appear to be explained simply by knowing how stress has evolved over the past century or two based on stress changes associated with earthquake slip and interseismic loading. No knowledge of the stress field prior to the relatively short study period appears to be required. Studies of changes in Coulomb stress, which considers both shear- and normal-stress changes to quantify whether faults have been pushed closer to

(positive Coulomb stress change) or further away from (negative Coulomb stress change) failure by nearby earthquakes, have shown to be particularly revealing (e.g., Jaeger and Cook, 1979; Stein and Lisowski, 1983; King et al., 1994). For example, Stein et al. (1994) show that the 1933 M_w = 6.4 Long Beach and 1952 M_w = 7.3 Kern County, California earthquakes combined to increase Coulomb stress at the eventual hypocenter of the 1971 M_w = 6.7 San Fernando earthquake, which in turn increased Coulomb stress at the eventual hypocenter of the 1994 M_w = 6.7 Northridge quake. Coseismic stress changes associated with earthquakes can also unload nearby faults and potentially induce a period of seismic quiescence (e.g., Scholz, 1988, Harris and Simpson, 1996, 1998). For example, the 1906 San Francisco earthquake initiated a period of seismic quiescence in the Bay area in which only 2 $M_w \geq 6$ earthquakes occurred in the 75 years following the great quake compared to 15 in the 75 years prior (Bakun, 1999).

Deng and Sykes (1997a, 1997b) explored the relationship between seismicity and Coulomb stress changes in southern California over the past two centuries by considering not only sudden stress changes due to all major earthquakes, but also due to the steady, long-term accumulation of stress resulting from the relative motion of the North American and Pacific plates. They found that 95% of 37 $M \geq 6$ earthquakes that occurred in southern California between 1812 and 1995 and 85% of 138 $M \geq 5$ earthquakes from 1932 to 1995, occurred on faults with Coulomb stress increases from major earthquakes and interseismic loading since 1812. This study did not, however, take into account the process of postseismic relaxation of a viscous lower crust and upper mantle which, following major earthquakes, can transfer significant stress upward to the seismogenic shallow crust (e.g., Pollitz, 1995; Freed and Lin, 1998, Chéry et al., 2001; Marsan and Bean, 2003). Here we expand on the calculations by Deng and Sykes (1997a, 1997b) by considering stress transfer due to postseismic relaxation and by calculating interseismic stress rates from strain rates calculated directly from surface velocities from the Southern California Earthquake Center (SCEC) Crustal Motion Map (Version 3) (http://epicenter.usc.edu/cmm3, Shen et al., 2003). By calculating stress rates from surface velocities we avoid any assumptions regarding mechanisms of interseismic strain accumulation. The limitation of such an approach is that we assume that accumulating interseismic strains are uniform with depth through the seismogenic upper crust.

The calculations consider how stress in southern California has been modified by 21 $M_w \geq 6.5$ events since 1812 (Table 1, black focal mechanisms in Figure 1). These represent all large events over the past two centuries in which a reasonable characterization of the slip distribution has been determined. Except were noted in Table 1, we use the same slip distributions as Deng and Sykes (1997a, 1997b). In addition to the $M_w \geq 6.5$ events, we consider how stress changes over the past two centuries resolve themselves on an additional 53 $6.0 \leq M_w < 6.5$ events (Table 2, blue focal mechanisms in Figure 1) (Kagan et al., 2006). We do not consider how these smaller events subsequently influence the regional stress field as they only perturb the stress locally (10s of km). Our study focuses on the evolution of stress on the broad landscape of southern California and how the hypocenters of historic quakes have been influenced by these stress changes.

Year	Location	Lat.	Lon.	M_w	Strike/Dip/Rake	Ref.	$\Delta\sigma_c$ Co. (MPa)	$\Delta\sigma_c$ Post. (MPa)	$\Delta\sigma_c$ Inter. (MPa)	$\Delta\sigma_c$ Net (MPa)
1812	Wrightwood	34.37	-117.65	7.50	295/90/180	1	0.000	0.000	0.000	0.000
1857	Fort Tejon	35.30	-119.80	8.20	321/90/180	1	0.033	0.008	0.509	0.550
1872	Owens Valley	36.70	-118.10	7.30	340/80/-171	1	0.004	0.016	0.121	0.141
1892	Laguna Salada	32.55	-115.63	7.20	328/90/180	1	0.017	0.040	0.923	0.979
1899	San Jacinto	33.80	-117.00	6.70	309/90/180	2	0.120	0.167	0.655	0.942
1915	Volcano Lake	32.33	-115.18	6.60	312/88/180	2	-0.562	0.188	1.397	1.023
1918	San Jacinto	33.80	-117.00	6.80	150/87/-176	2	0.368	0.188	0.878	1.434
1927	Lompoc (T)	34.35	-120.90	6.60	340/66/95	3	-0.046	-0.042	0.039	-0.049
1934a	Laguna Salada	32.25	-115.50	6.50	311/88/180	2	0.181	0.436	1.493	2.111
1934b	Co. River Delta	32.00	-114.75	7.00	317/89/180	2	0.133	0.056	1.199	1.388
1940	Imperial Valley	32.87	-115.48	7.00	325/90/180	1	0.122	0.314	2.985	3.421
1947	Manix	34.98	-116.55	6.50	65/85/8	2	-0.040	-0.176	1.245	1.030
1952	Kern County (T)	35.00	-119.02	7.50	51/75/25	1	2.991	-0.304	-0.384	2.303
1968	Borrego Mountain	33.19	-116.13	6.50	311/78/179	2	0.068	0.106	2.143	2.318
1971	San Fernando (T)	34.41	-118.40	6.60	255/53/75	2	1.633	-0.456	-0.320	0.857
1987	Superstition Hills	33.01	-115.85	6.60	303/90/180	2	0.074	0.218	1.378	1.670
1992a	Landers	34.20	-116.44	7.30	340/74/-176	1	-0.164	-0.010	2.514	2.339
1992b	Big Bear	34.20	-116.83	6.50	48/90/0	1	-0.467	0.022	1.925	1.480
1994	Northridge (T)	34.27	-118.54	6.70	128/33/106	1	0.016	-0.018	0.160	0.158
1999	Hector Mine	34.59	-116.27	7.20	336/80/174	4	-0.325	-0.009	1.047	0.713
2003	San Simeon (T)	35.71	-121.10	6.60	296/50/90	5	-0.035	0.053	-0.313	-0.296

Table 1. $M_w \geq 6.5$ earthquakes in southern California over the past two centuries used to calculate changes to the stress field and the stress changes at their respective hypocenters just prior to rupture (see Figure 1). A (T) after the location name denotes a event which has a significant thrust component, in which case $\mu' = 0.8$ is assumed, otherwise $\mu' = 0.4$ is assumed. Lat/Lon indicates the latitude and longitude of the hypocenters of these events. Strike/Dip/Rake indicates the sense of slip at the hypocenter. $\Delta\sigma_c$ Co is the change in coseismic Coulomb stress at the hypocenter due to previous earthquakes. $\Delta\sigma_c$ Post is the change in Coulomb stress due to viscoelastic relaxation associated with previous events. $\Delta\sigma_c$ Inter is the change in Coulomb stress due to the regional strain rate field from GPS from 1812 to just before rupture. $\Delta\sigma_c$ Net is the sum of coseismic, postseismic, and interseismic Coulomb stress changes from 1812 to just prior to rupture. References numbers refer to the source for both hypocenter location and slip distribution: 1. Deng and Sykes, 1997a, 2. Deng and Sykes, 1997b, 3. Helmberger et al., 1992, 4. Hurst et al., 2000, 5. Hardebeck et al., 2004. Notes: For the 1952 Kern County earthquake we use the hypocenter fault plane orientation from Lin and Stein (2004) and a depth of 20 km. For the 1971 San Fernando earthquake we use the hypocenter fault plane orientation from Heaton (1982). Coseismic stress change due to the 1899 event on the 1918 San Jacinto hypocenter is neglected due to errors caused by overlap of these events.

2.0 Interseismic Strain Accumulation

Interseismic strain rates have previously been calculated by Jackson et al. (1997) from the 1st version of the SCEC velocity field (287 velocity vectors), finding that high shear strain rates were observed not only near the major faults, but also in regions surrounding previous earthquakes, such as the 1992 Landers, 1979 Imperial Valley, and the 1952 White Wolf events. Working with an increased number of GPS stations, Wdowinski et al. (2001) utilized the 2nd version of the SCEC velocity field (363 velocity vectors), where most of the data was concentrated around the SAF. They found high interseismic strain rates to be localized along a dozen sub-parallel belts in a narrow zone around the San Andreas that correlated well with the active geologic fault segments and concentrated zones of microseismicity. High shear strain rates (0.3-0.95 μstrain/year) were observed

northward and southward of the SAF's big bend, whereas the big bend itself was characterized by a diffuse low magnitude shear strain rate. Here we utilize the 3rd version of the SCEC Crustal Motion Map (http://epicenter.usc.edu/cmm3/), which provides a broader view of surface motions (840 velocity vectors), including the ECSZ, enabling a more regional understanding of interseismic strain rates (Figure 2; note that for clarity this figure shows only a subset of the observed velocity vectors). The great density of these measurements minimizes errors associated with interpolating strain rates between station locations.

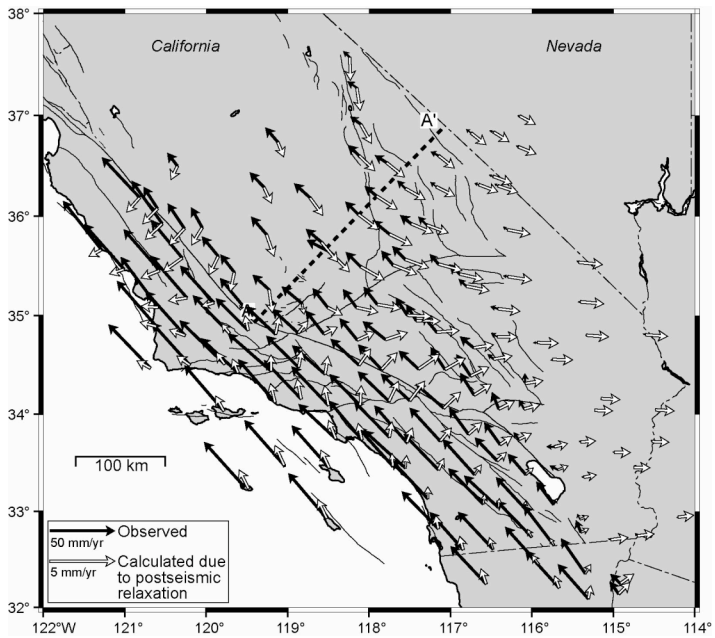

Figure 2. SCEC 3 observed surface velocities and calculated velocities in 2003 based on postseismic relaxation from historic earthquakes (Table 1, but not 1992, 1999, and 2003 events). Note that the observed velocities are plotted on a scale that is 10 times bigger than the postseismic relaxation velocities. For clarity, only a subset of the SCEC 3 velocity set is shown.

The advantage of directly calculating strain rates from the observed velocity field is that it does not require us to understand the mechanics of interseismic strain accumulation. However, if we superimpose stresses derived from interseismic strain rates with those derived from separate calculations of postseismic relaxation, a problem could arise if the velocity field contains substantial contributions from those same relaxation processes. If such is the case, stress changes associated with postseismic relaxation would be exaggerated. The first step in our analysis is thus to determine the extent to which current surface velocities in southern California are influenced by postseismic relaxation associated with earthquakes that have occurred in the past 200 years. Contributions of pre-1812 postseismic processes to current surface velocities, such as due to a background strain rate associated with repeated earthquake cycles (Savage and Lisowski, 1998; Segall, 2002; Dixon et al., 2003; Johnson and Segall, 2004; Kenner and Simons, 2005; Hetland and Hager, 2005), is of no concern since these contributions will not be duplicated by our postseismic calculations.

Viscoelastic relaxation contributions are calculated using the code Visco1D developed by Pollitz (1997), which is based on the normal mode representation of deformation in a layered spherical Earth with elastic-viscoelastic coupling, including the effects of compressibility and gravitational coupling. Fault segments are modeled as planar rectangular patches of constant strike, dip, rake, and slip, spanning the rupture surface of each earthquake. The primary unknown in these calculations is the assumed viscosity

structure. Analyses of postseismic deformation following the 1992 Landers and 1999 Hector Mine earthquakes suggest that after several years of early fast strain rates, the effective viscosity of the southern California lithosphere can be described with an upper mantle viscosity of the order of 10^{19} Pa s and a lower crustal viscosity 3 times that level (Pollitz et al., 2000, Freed and Bürgmann, 2004). This is consistent with the effective viscosity of the San Francisco Bay region inferred from observations of postseismic deformation in the decades following the 1906 San Francisco quake (Kenner and Segall, 2003; Pollitz and Nyst, 2005) and with long-term relaxation times (25 to 40 years) associated with analytical viscoelastic coupling models associated with the velocity field around the big bend in southern California (Thatcher, 1983; Savage and Lisowski, 1998). In all of our viscoelastic calculations we use a viscosity of 1.2×10^{19} Pa s for the mantle and 3.6×10^{19} Pa s for the lower crust, the same rheology inferred by Pollitz and Nyst [2005] for the San Francisco region.

The SCEC 3 velocity field had been constructed ignoring the first year and a half after the Landers quake (and all post-Hector Mine data, Shen et al., 2003), but postseismic analyses suggest that relaxation continued to influence the velocity field from 1994 to 1999 (Pollitz et al., 2000, Freed and Bürgmann, 2004). Thus, our initial calculation estimated the average surface velocity due to post-Landers relaxation from 1994 to 1999, which was then removed from the SCEC velocity field. The peak average post-Landers velocity over this time period was found to be as much as 15 mm/yr within 20 km of the fault and 3 mm/yr within a 100 km distance, representing a significant portion of the SCEC velocities in the ECSZ. We subtracted these velocities from the SCEC 3 velocity field to form a corrected version more likely representative of long-term interseismic velocities in southern California.

We then calculated the collective contributions from viscoelastic relaxation from 1812-2000 earthquakes (Table 1; not including Hector Mine, which is not part of the SCEC data) to southern California surface velocities in 2000. We found these velocities to be relatively small, with peak velocities less than 2 mm/yr, much smaller than those observed by GPS (note the factor of 10 difference in plotting scales in Figure 2). In addition, the velocity pattern associated with collective postseismic relaxation shows little correspondence to the observed velocity field. From this we conclude that postseismic relaxation associated with historic earthquakes does not significantly influence the present day velocity field and by extension, has little influence on interseismic strains derived from these velocities.

Having concluded that the SCEC 3 velocity field (minus Landers contributions) does not have a substantial component of postseismic relaxation from events occurring over the past two centuries, we proceeded to calculate associated interseismic strain rates. To calculate interseismic strain rates, each velocity vector was resolved into fault-parallel and fault-perpendicular components, where the fault parallel direction is based on the average azimuth of the SAF (N40°W). We then linearly interpolated the velocity data to an evenly spaced grid with increments of 0.1 degrees across the region using a weighted nearest neighboring scheme, which dampens any locally sharp velocity contrasts. For grid points outside of the SCEC 3 region, we extrapolated the velocity field based on a

fixed North America plate and a Pacific plate with a velocity of 48 mm/yr. Because of the dense coverage of the SCEC 3 data set, only a few outlying regions required assumptions of relative plate motions.

We then triangulate the evenly spaced grid points (with a resolution of 0.1 degrees) using Delaunay triangulation (e.g., Shewchuk, 1996), and the strain tensor is determined for each triangle using minimum norm least squares. The resolved maximum shear-strain rate across southern California inferred from the velocity field is shown in Figure 3. Interseismic shear strain is concentrated along the SAF through southern California, though the San Jacinto Fault shares strain with the SAF in the south. Strain rates along the creeping section of the SAF (above 36°N) are not well resolved because of a lack of stations on the west side of the fault, and below 33°S for similar reasons (creeping segments in these regions also induce anomalous interpretations of strain rate). These results are in general agreement with the magnitude of strain rates inferred from SCEC 1 (Jackson et al., 1997) and SCEC 2 (Wdowinski et al., 2001), though the present analysis has a substantially larger array of geodetic measurements from which to more accurately infer the strain field. Relatively high strain rates in the vicinity of the Landers quake may suggest that the contribution to the velocity field due to post-Landers relaxation was probably not completely removed by our correction.

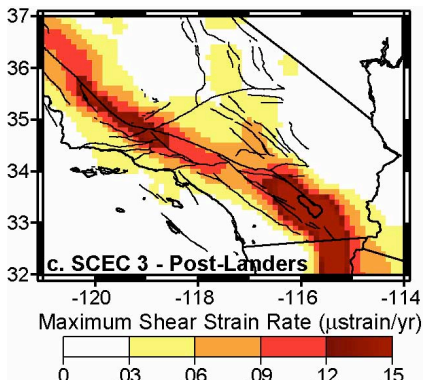

Figure 3. Maximum shear strain rates based on SCEC 3 velocities minus contributions from Landers postseismic relaxation (see text).

3.0 The Evolution of Stress

We focus our study on the calculation of Coulomb stress changes, which is based on the concept of a critical Coulomb failure stress, σ_c, in which

$$\sigma_c = \tau - \mu(\sigma_n - p), \tag{1}$$

where τ is shear stress parallel to the slip direction of a fault, σ_n is fault-normal (or clamping) stress, p is pore fluid pressure, and μ is the coefficient of friction (Jaeger and Cook, 1979; Scholz, 2002). The Coulomb failure criterion was developed in the laboratory where the absolute applied shear and normal stresses on rock specimens could be measured. While the absolute stress field is difficult to determine, as it depends on a long, unkown history of earthquakes and other dynamic processes, stress changes due to historic coseismic, postseismic, and interseismic processes can be estimated. We thus rewrite the equation for Coulomb stress change in the form,

$$\Delta\sigma_c = \Delta\tau - \mu'\Delta\sigma_n, \tag{2}$$

where Δ represents change in stress and μ' is the apparent friction, which takes into account reductions in friction due to pore pressure changes (e.g., Harris, 1998). This equation implies that a fault will be brought closer to failure if the shear stress parallel to the slip vector is increased or the normal stress is decreased (positive change in Coulomb

stress), or will be brought farther away from failure if these components are of the opposite sign (negative change in Coulomb stress).

We calculate the evolution of Coulomb stress in southern California by considering contributions from coseismic, postseismic, and interseismic stress changes since the 1812 Wrightwood earthquake. Our objective is to determine the role of each of these mechanisms in the evolution of stress since 1812 and to determine how stress at the hypocenters on subsequent earthquake rupture planes were influenced. Several studies suggest that aftershocks of thrust faults are sensitive to normal stress changes, implying a relatively high apparent friction coefficient for thrust faults, perhaps about 0.8 (e.g., Stein and Ekström, 1992; Shearer, 1997; Hardebeck et al., 1998; Parsons et al., 1999). In contrast, evidence favors low friction for strike-slip faults with significant cumulative slip, such as the San Andreas, for which $\mu' < 0.4$ (Zoback et al., 1987; Harris et al., 1995; Parsons et al., 1999; Toda and Stein, 2002). Correspondingly, our Coulomb stress calculations assume a constant effective friction of $\mu' = 0.8$ when calculating stress changes on thrust faults and of $\mu' = 0.4$ for strike-slip faults. Unless stated otherwise, all of our calculations assume a hypocenter depth of 8 km, the average nucleation depth of the earthquakes considered.

3.1 Coseismic Stress Changes

Coseismic Coulomb stress changes are calculated for all $M_w \geq 6.5$ events since 1812 (Table 1) based on the method of Pollitz (1996) and slip distributions based on previous analyses (Deng and Sykes, 1997a, 1997b; Helmberger et al., 1992; Hurst et al., 2000; and Hardebeck et al., 2004; see Table 1 for respective sources). Figure 4 shows the results of cumulative coseismic Coulomb stress changes as resolved on right-lateral strike-slip faults parallel to the general trend of the SAF (N40°W). This is a reasonable approximation of how most strike-slip faults in the region have been coseismically loaded by previous events. This figure focuses on six time periods: just after the 1812 M_w=7.5 Wrightwood quake (Figure 4a), just after the 1857 M_w=8.2 Fort Tejon quake (Figure 4b), just after the 1892 M_w=7.2 Laguna Salada quake (Figure 4c), just after the 1952 M_w=7.5 Kern County quake (Figure 4d), just after the 1992 M_w=7.3 Landers quake (Figure 4e), and the cumulative change in Coulomb stress due to all considered events as of the end of 2005 (Figure 4f). Given the uncertainty in the friction and pore pressure inherent to faults (e.g. Beeler et al., 2000), we also plot coseismic Coulomb stress for the case where $\mu' = 0.0$ (i.e., shear-stress change only) in Supplemental Figure 1.

Figure 4 shows that the coseismic stress field in southern California is dominated by stress changes imparted by the 1857 Fort Tejon quake, by far the largest event to occur over the past 200 years. Coulomb stress has been increased to the northwest (Parkfield region) and to the southeast where the San Bernardino Mountain and Coachella Valley segments of the SAF and the San Jacinto fault lie. Both of these regions are marked by a large number of events since 1857. The 1857 quake also led to a stress shadow (region of Coulomb stress decrease) for similarly aligned faults to the west and east of the rupture zone, most notably across the southern portion of the Eastern California Shear Zone. The 1872 Owens Valley rupture further to the north along the ECSZ lies in an area of small positive stress change. The stress shadow may explain why few events have occurred in

the southern ECSZ from 1857 until the recent events of the 1990s, but faults in the ECSZ also have long (1000s of years) recurrence intervals (Rockwell et al., 2000) and therefore the recent lack of large events may not be remarkable. Unlike the documented reduction of seismicity within the stress shadow induced by the 1906 San Francisco quake (Bakun, 1999), seismicity in the ECSZ prior to the 1857 event is not well constrained. Thus, it is difficult to draw firm conclusions regarding the significance of the Fort Tejon stress shadow. The cumulative effect of coseismic Coulomb stress changes (at 8 km depth) over the past two centuries is stress relief over 79% of southern California, compared to stress increases over 21% of the region.

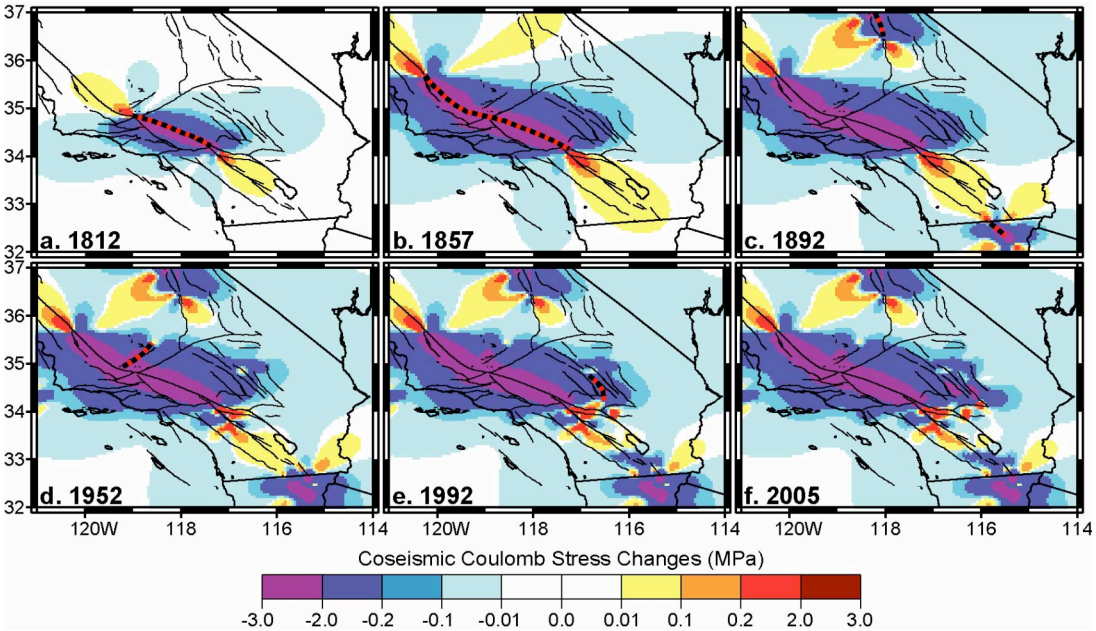

Figure 4. Calculated coseismic Coulomb stress changes resolved at 8 km depth on vertical right-lateral strike-slip faults striking parallel to the San Andreas fault (N40°W) with apparent friction μ´ = 0.4 at various times over the past two centuries: just after the (a) 1812 M_w=7.5 Wrightwood quake, (b) 1857 M_w=8.2 Fort Tejon quake, (c) 1892 M_w=7.2 Laguna Salada quake, (d) 1952 M_w=7.5 Kern County quake, (e) 1992 M_w=7.3 Landers quake, and (f) cumulative change in Coulomb stress due to all considered events as of the end of 2005. Each panel shows the major earthquake rupture surface (black and red dashed line) that occurred that year (none for 2005).

We have calculated the coseismic Coulomb stress change as resolved on the sense of hypocentral slip (Table 1, column 6) for each historic earthquake over the past two centuries. The cumulative coseismic stress change for each event just before rupture due to all previous events is summarized in Table 1 (column 8). Coseismic Coulomb stress changes could not be accurately calculated at several events as they occurred very close to previous rupture surfaces and calculated stress changes vary greatly with small variations in model parameters, as indicated with dashed lines in Table 1. A summary of these tables finds that 56% of hypocenters experienced an increase in Coulomb stress due to coseismic slip of earlier events. This percentage supports the argument that earthquake occurrence is controlled by factors other than coseismic Coulomb stress changes alone. This conclusion is consistent with the findings of Kagan et al. (2005)–Deng and Sykes (1997a, 1997b) did not analyze coseismic stress changes alone.

3.2 Postseismic Stress Changes

Following large earthquakes, coseismic stress changes are further modified by relaxation of a viscous lower crust and upper mantle, which serves to transfer stress from these warm regions both upwards to the seismogenic crust and outwards across a broader region. Calculations of postseismic stress changes were carried out using the same numerical code and assumptions discussed in section 2.0. The influence of postseismic relaxation of a viscoelastic lower crust and upper mantle on Coulomb stress changes associated with right-lateral strike-slip faults parallel to the SAF is shown in Figure 5. (Supplemental Figure 3 show these time frames for an assumed frictional values of $\mu' = 0$.) A comparison of coseismic (Figure 4) and postseismic (Figure 5) Coulomb stress changes shows that both fields are dominated by the 1857 Fort Tejon quake with both mechanisms leading to stress increases at the ends of the Fort Tejon rupture and stress decreases to either side for strike-slip events parallel to the SAF. In general, postseismic stress changes further intensify and widen coseismic stress changes, but rapidly rebuilds stress along rupture planes. Table 1 (column 9) and Table 2 (column 8) summarize the postseismic Coulomb stress changes due to relaxation associated with previous events imparted at the hypocenter of each earthquake. A summary of these tables finds that 73% of hypocenters experienced an increase in postseismic Coulomb stress, showing a modestly greater correlation between postseismic Coulomb stress increases and the location of subsequent hypocenters than was observed in the coseismic calculations.

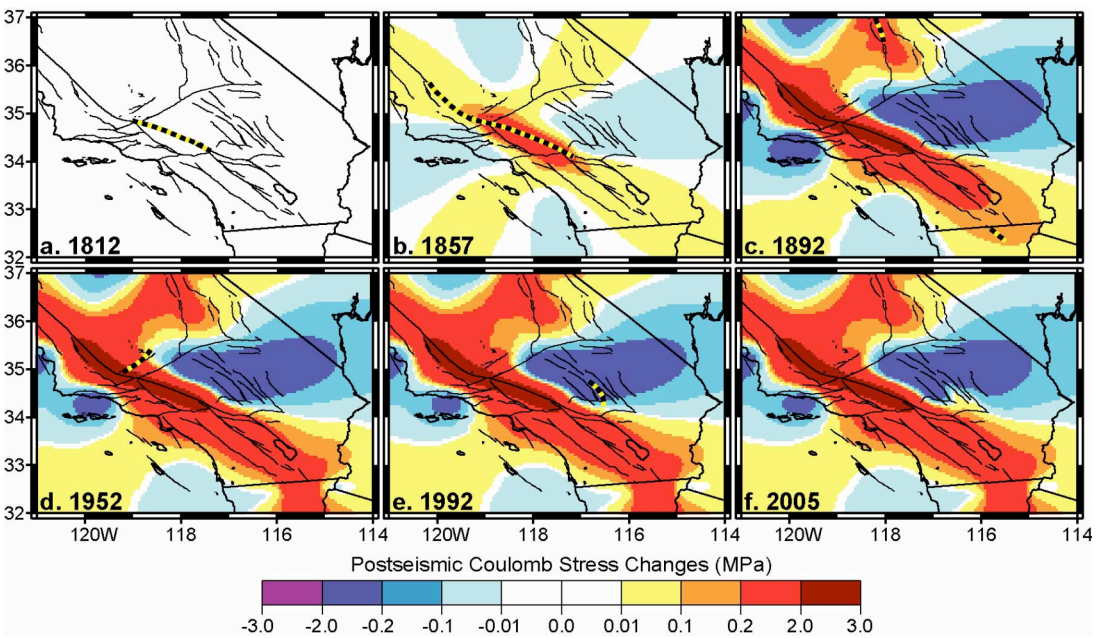

Figure 5. Same as Figure 4, but for calculated postseismic Coulomb stress changes.

The addition of postseismic stress changes greatly magnifies the coseismic stress changes to the northwest and southeast of the Fort Tejon rupture and greatly increases the magnitude and extent of the stress shadow imparted by the For Tejon quake, especially over the ECSZ. (see also Pollitz and Sacks, 1992; Rydelek and Sacks, 2001). Postseismic stress changes lead to a decrease in the area of reduced Coulomb stress (at 8 km depth)

from 79% associated with coseismic stress changes alone to 69% within the study region when postseismic stress changes are also taken into account.

Amongst the larger events, the occurrence of the 1947 Manix, 1992 Landers, 1992 Big Bear, and the 1999 Hector Mine earthquakes remain difficult to explain in terms of net Coulomb coseismic and postseismic stress changes, as the respective hypocenters all experience net coseismic plus postseismic Coulomb stress decreases, primarily from the Fort Tejon stress shadow. It is not clear whether coseismic changes associated with the Landers quake encouraged or inhibited rupture of the Hector Mine earthquake, as slight changes in modeling assumptions can flip the sign of coseismic stress changes (see also Harris and Simpson, 2002). Postseismic relaxation following the Landers earthquake does, however, increase Coulomb stress at the hypocenter of the Hector Mine event by ~0.8 MPa (see also Freed and Lin, 2001; Zeng, 2001; Pollitz and Sacks, 2002). Despite the fact that this postseismic stress increase associated with the Landers quake is not sufficient to overcome the stress shadow induced by the 1857 earthquake, the Hector Mine ruptured only 7 years after the Landers quake. Again , this raises the possibility that the rate of Coulomb stress change may be more important than the magnitude (Toda et al., 2005, Parsons et al. , 2000).

3.3 Interseismic Stress Changes

Interseismic Coulomb stress change rate was calculated based on the inferred interseismic strain rate (Figure 3) using the time derivative of equations 3-1 to 3-3 in Turcotte and Schubert (1980). Figure 6 shows the resulting interseismic Coulomb stress rate for right-lateral strike-slip faults striking parallel to the SAF (N40°W). Peak stressing rates of >2 KPa yr^{-1} across a band ~200 km wide along the SAF is consistent with differential stresses found by Parsons (2006), who used GPS velocities to drive a model of crustal deformation. This band is much broader and the magnitude of stressing rates much lower than that found from models of loading due to deep slip (e.g., Smith and Sandwell, 2003, 2006). As pointed out by Parsons (2006), either modeling approach can satisfy surface velocity constraints, thus leaving the actual mechanisms of strain accommodation unknown.

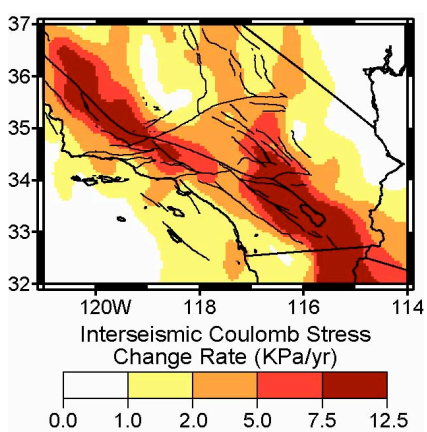

Figure 6. Interseismic Coulomb stress rates resolved on vertical right-lateral strike-slip faults striking parallel to the San Andreas fault (N40°W). Calculations are based on an assumed effective friction of 0.4 and are derived from the shear strain field shown in Figure 6.

The pattern of the regional stressing rate closely resembles the maximum shear strain rate. As interseismic shear represents the driving load of the SAF system, it is not surprising that the interseismic Coulomb stress rate is only positive. Shear stress rates are maximized along the Cholame and Mojave segments of the SAF in the north and along the Coachella Valley segment and the San Jacinto fault in the south, with the presence of the big bend causing a broadening of the high-stress zone to encompass the ECSZ through the middle of the region. Though these rates are relatively

small on a yearly basis compared to stress changes induced by earthquakes, their relentless application dominates the stress field in the long term. The interseismic stress rate calculations are inaccurate at the creeping sections of the SAF to the north of 36°N and south of 32.5°S. Both of these regions are marked by a sharp discontinuity in the strain rate field, which are not captured by the strain field we derived from the sparsely distributed GPS observations.

While one may expect to find that Coulomb stress is increased at all hypocenters due to interseismic loading, as one would surmise that all faults in southern California arise from the long term motions of the Pacific and North American plates, that is not the case for several thrust events, including the 1952 Kern County and 1971 San Fernando hypocenters that are calculated to be unloaded by the interseismic stressing rate we deduced from the GPS velocities. These hypocenters were, however, both significantly loaded coseismically by the 1857 Fort Tejon quake to the extent that the net Coulomb stress change since 1812 at each of these hypocenters is positive. If these calculations are correct, it would suggest that both events are responses to Fort Tejon type events on the San Andreas Fault, as opposed to the interseismic stress changes. For thrust event such as these the assumption of an apparent friction (in this case 0.8) greatly influences calculated interseismic Coulomb stress changes. In fact, Coulomb stresses at the hypocenters of both of these events is calculated to increase in response to interseismic loading if the apparent friction is assumed to be low (< 0.4). This is also true for the loading of the hypocenters of the 1983 Coalinga and 2003 San Simeon events.

3.4 Net Stress Changes

Assuming a neutral stress state just prior to the 1812 Wrightwood earthquake, we added interseismic stress (stress rate multiplied by time since 1812) to that calculated from coseismic and postseismic stress changes, providing a view of the net evolution of stress through the 19th and 20th centuries in southern California (Figure 7). The addition of interseismic stresses increase stress throughout the region for strike-slip faults similarly oriented to the SAF. Interseismic stress increases add to large positive coseismic and postseismic stress along the southern portion of the SAF system (southeast of the Fort Tejon rupture), generating a region of significant unrelieved stress since 1812. This evolution has critically loaded the San Bernardino Mountain and Coachella Valley segments of the SAF and the San Jacinto Fault. Stress on the southernmost San Andreas segment, which has not ruptured since ~1680 (Sieh et al., 1989), has increased on the order of 3 MPa due to coseismic, postseismic, and interseismic stress changes since 1812 (Figure 7f). Due to interseismic stress rates alone, stress on this segment has increased by more than 5 MPa since the last rupture in 1680. Despite the fact that this southern region is the most seismically active in southern California over the past 100 years, with more than two dozen $M_w \geq 6.0$ events, this seismicity has done little to relieve the stress that has developed both from interseismic loading and the 1857 Fort Tejon earthquake and subsequent postseismic relaxation.

In contrast, interseismic stress increases have worked to erode the large stress shadow cast by the 1857 Fort Tejon quake over the ECSZ (compare Figures 5f and 7f). The result is a reduction of the area within southern California characterized by a post-1812

decrease in Coulomb stress from 69% from coseismic plus postseismic changes, to only 34% after interseismic loading is considered. At current interseismic rates, the stress shadow cast by the Fort Tejon quake and associated postseismic relaxation should be erased within the next several decades. If this shadow has been responsible for decreased seismicity in this portion of the ECSZ, then this region may experience a significant increase in seismicity in the decades to come. Though it is only speculation, it is possible that the quakes that occurred in the southernmost ECSZ in the 1990s (Joshua Tree, Landers, Big Bear, Hector Mine) could mark a beginning of a new cycle of seismicity in the region. Interseismic stress increases are also working to reload the Fort Tejon rupture surface, though it will take more than another century for the stress levels on this segment of the SAF to reach pre-1812 levels.

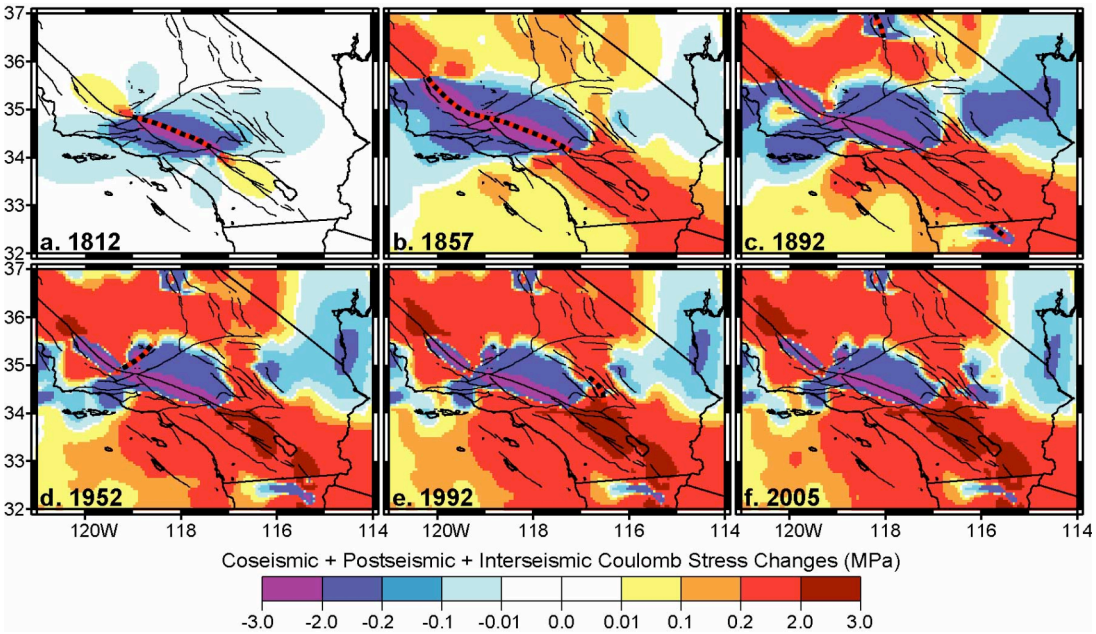

Figure 7. Same as Figure 4, but for calculated coseismic plus postseismic plus interseismic Coulomb stress changes.

As expected, most events have a net Coulomb stress increase. Several earthquakes in our catalog appear to nucleate despite their hypocenters having experienced a net Coulomb stress decrease between 1812 and the time of their rupture. These include the 1927 Lompoc, the 1952 Bakersfield, the 1983 Coalinga, the 2003 San Simeon, and several small 19th century events. Almost all of these exceptions are thrust events. As discussed above, the stresses at these hypocenters are very sensitive to assumptions of apparent friction. With the exception of a couple of early 19th century events (1827, 1855), where slip characteristics are not well constrained, the 1952 Bakersfield quake is the only modern day strike-slip event to have occurred with a net decrease in Coulomb stress. The 1952 Bakersfield earthquake was an aftershock of the Kern County earthquake, occurring only 8 hours after the mainshock despite a calculated decrease in Coulomb stress due to the Kern County rupture. The rake of this earthquake, which has a significant influence on resolved stresses at the hypocenter, is poorly resolved, which could account for this discrepancy. Choosing the northeast-striking nodal plane leads to a

positive coseismic Coulomb stress change as well. It is also possible that another mechanism such as dynamic triggering may have played a roll in the triggering of this aftershock.

4.0 Conclusions

We calculated the evolution of Coulomb stress in southern California due to $M_w \geq 6.5$ earthquakes since 1812 due to interseismic strain accumulation, coseismic slip, and postseismic relaxation of a viscoelastic lower crust and upper mantle. The calculations reveal the overwhelming influence of the 1857 $M_w = 8.2$ Fort Tejon earthquake on the evolving stress field of southern California. Stress changes associated with this earthquake cast a wide stress shadow decreasing the load on faults in the region throughout the 19th century, while greatly increasing stresses to the north (Parkfield region) and the southern SAF system to the south. These stress changes were greatly enhanced by subsequent postseismic relaxation through the beginning of the 20th century. Interseismic stress accumulation further increased loading on most of the strike-slip faults in southern California, adding to stress increases from coseismic and postseismic stress changes, and working to erode the stress shadow in the ECSZ. Postseismic relaxation also occurs on a smaller scale following each earthquake, though only the $M_w \geq 7$ events significantly influence the regional distribution of stress. Today southern California is characterized by unrelieved stress increases along the San Bernardino Mountain and Coachella Valley segments of the SAF and the San Jacinto fault zone.

Our results demonstrate the importance of postseismic viscoelastic relaxation in the redistribution of stress following large earthquakes, but also reveal that such processes are near completion and thus do not significantly influence the regional velocity field presently observed in southern California. Calculations show that, with the exception of the 1992 Landers and 1994 Hector Mine quakes, postseismic relaxation of previous quakes over the past two centuries account for less than 2 mm/yr of currently observed surface velocities.

We also calculated the evolution of Coulomb stress at the hypocenter of $M_w \geq 6$ earthquakes since 1812. We found that coseismic Coulomb stress changes increased the stress at 56% of subsequent historic hypocenters, indicating that earthquake occurrence is not uniquely determined by coseismic stress changes. This percentage rises to 70% when postseismic stress changes are also considered. Not surprisingly, interseismic stress accumulation is found to load most faults in the region, but not all. Some hypocenters, such as those associated with the 1952 Kern County and 1971 San Fernando quakes, are modestly unloaded by interseismic strains used in our model calculation. These results could arise from our assumption of high apparent friction on thrust faults, limitations that arise from inferring strain from a limited set of GPS velocities, or they could imply that such events only occur in response to the manner in which major events such as the 1857 Fort Tejon quake reorganize the stress field. Incorporating interseismic loading in the stress-change calculations modestly increases the percentage of events that experienced Coulomb-stress increase since 1812 to 73 %.

While most historic earthquakes in southern California incurred Coulomb stress increases due to prior earthquakes that occurred since 1812, this finding does not prove that fault-interaction stresses play a dominant role in the distribution of earthquakes in space and time. Nonetheless, we believe it is appropriate to incorporate knowledge about

the evolution of stress derived from physical models of interseismic, coseismic and postseismic deformation into time-dependent earthquake hazard estimates of active fault systems.

4.0 Publications resulting from this grant

Freed, A. M., S. T. Ali, and R. Bürgmann, Stress Evolution in Southern California for the Past 200 Years From Coseismic, Postseismic, and Interseismic Processes, *Geophys. J. Inter.,* doi: 10.1111/j.1365-246X.2007.03391, 2007.

References

Bakun, W. H., 1999. Seismic activity of the San Francisco Bay region, *Bull. Seismol. Soc. Am., 89*, 764-784.

Beeler, N. M., R. W. Simpson, S. H. Hickman, and D. A. Lockner, 2000. Pore fluid pressure, apparent friction, and Coulomb failure, *J. Geophys. Res.*, *105*(B11), 25,533–25,542.

Chéry J, S. Merkel, and S. Bouissou, 2001. A physical basis for time clustering of large earthquakes, Bull Seismo. Soc. Am., 91, 1685-1693.

Deng, J., and L. Sykes, 1997a. Evolution of the stress field in southern California and triggering of moderate-size earthquakes: A 200-year perspective, *J. Geophys. Res., 102*, 9859-86.

Deng, J,, L. R. Sykes, 1997b. Stress evolution in southern California and triggering of moderate-, small-, and micro-size earthquakes, *J. Geophys. Res., 102*, 24411-24435.

Deng, J., M. Gurnis, H. Kanamori, and E. Hauksson, 1998. Viscoelastic flow in the lower crust after the 1992 Landers, California, earthquake, *Science, 282*, 1689-92.

DeMets, C., and T. Dixon, 1999. New kinematic models for Pacific-North America motion from 3 Ma to present, 1: Evidence for steady motion and biases in the NUVEL-1A model, *Geophys. Res. Lett., 26*, 1921-1924.

Dieterich J. H., 1994. A constitutive law for rate and of earthquake production and its application to earthquake clustering. *J. Geophys. Res. 99*, 2601–2618.

Dixon, T. H., E. Norabuena, and L. Hotaling, 2003. Paleoseismology and Global Positioning System; earthquake-cycle effect and geodetic versus geologic fault slip rates in the Eastern California Shear Zone, *Geology, 31*, 55-58.

Felzer, K. R., and E. E. Brodsky, 2005. Testing the stress shadow hypothesis, *J. Geophys. Res.*, *110*, B05S09, doi:10.1029/2004JB003277.

Felzer, K. R. and E. E. Brodsky, 2006. Decay of aftershock density with distance indicates triggering by dynamic stress, Nature, 441, 735-738.

Freed, A. M., and J. Lin, 1998. Time-dependent changes in failure stress following thrust earthquakes, J. Geophys. Res., 103, 24,393-24,409.

Freed, A. M., and J. Lin, 2001. Delayed triggering of the 1999 Hector Mine earthquake by viscoelastic stress transfer, Nature, 411, 180-183.

Freed, A. M. and J. Lin, 2002. Accelerated stress buildup on the southern San Andreas Fault and surrounding regions caused by Mojave Desert earthquakes, *Geology, 30*, 571–574.

Freed, A. and R. Bürgmann, 2004. Evidence of power-law flow in the Mojave desert mantle, *Nature*, 430, 548-551.

Freed, A. M., 2005. Earthquake triggering by static, dynamic, and postseismic stress transfer, *Annu. Rev. Earth Planet. Sci., 33*, 335-367.

Freed, A. M., R. Bürgmann, E. Calais, J. Freymueller, and S. Hreinsdóttir, 2006. Implications of Deformation Following the 2002 Denali, Alaska Earthquake for Postseismic Relaxation Processes and Lithospheric Rheology, *J. Geophys. Res., 111*, B01401, doi:10.1029/2005JB003894.

Gomberg J., 1996. Stress/strain changes and triggered seismicity following the M_w7.3 Landers, California earthquake. *J. Geophys. Res.*, 101, 751-764.

Gomberg J, P. Bodin, K. Larson, and H. Dragert, 2004. Earthquake nucleation by transient deformations caused by the M = 7.9 Denali, Alaska, earthquake, *Nature*, 427, 621-624.

Hardebeck, J., J. Nazareth, and E. Hauksson, 1998. The static stress change triggering model; constraints from two southern California aftershock sequences, *J. Geophys. Res*., 103, 24,427-37.

Hardebeck, J. L., Boatwright J, Dreger D, et al., 2004. Preliminary report on the 22 December 2003, M6.5 San Simeon, California earthquake, Seismol. Res. Lett., 75(2), 155–172.

Harris, R. A., R. W. Simpson, and P. A. Reasenberg, 1995. Influence of static stress changes on earthquake locations in southern California, Nature, 375, 221– 224.

Harris, R. A, and R. W. Simpson, 1996. In the shadow of 1857-the effect of the great Ft. Tejon earthquake on subsequent earthquakes in southern California, *Geophys. Res. Lett.*, 23, 229-232.

Harris, R. A., 1998. Introduction to special section: Stress triggers, stress shadows, and implications for seismic hazard, *J. Geophys. Res., 103*, 24,347-24,358.

Harris, R. A, and R. W. Simpson, 1998. Suppression of large earthquakes by stress shadows: A comparison of coulomb and rate-and-state failure, *J. Geophys. Res.*, 103, 24,439-51.

Harris, R. A, and R. W. Simpson, 2002. The 1999 M-w 7.1 Hector Mine, California, earthquake: A test of the stress shadow hypothesis?, *Bull. Seismol. Soc. Am., 92*, 1497-1512.

Heaton, T. H., 1982. The 1971 San Fernando Earthquake - A double event, Bull. Seis. Soc. Am., 72 : 2037 -2062.

Helmberger, D. V., P. G. Somerville, and E. Garnero, 1992. The location and source parameters of the Lompoc, California, Earthquake of 4 November 1927, *Bull. Seismol. Soc. Am., 82*, 1678-1709.

Hetland, E. A., and B. H. Hager, 2005. Postseismic and interseismic displacements near a strike-slip fault: A two-dimensional theory for general linear viscoelastic rheologies, J. Geophys. Res., 110, B10401, doi:10.1029/2005JB003689.

Hodgkinson, K., R. Stein, and G. Marshall, 1996. The 1954 Rainbow mountain-Fairview peak-Dixie valley earthquake sequences: a triggered normal faulting sequence, *J. Geophys. Res*., 101, 25,459-25,472.

Hurst K. J., D. F. Argu, A. Donnellan, M. B. Heflin, D. C. Jefferson, G. A. Lyzenga, J. W. Parker, M. Smith, F. Webb, and J. F. Zumberge, 2000. The coseismic geodetic signature of the 1999 Hector Mine Earthquake, *Geophys. Res. Lett., 27*, 2733-2736.

Jackson, D. D., S. Zheng-kang, D. Potter, X-B Ge, and L-y Sung, 1997. Southern California Deformation, Science, 277, 1621-1622.

Jacoby, G. C. Jr., P. R. Shepard, K. E. Sieh, 1988. Irregular recurrence of large earthquakes along the San Andreas fault in southern California – Evidence from trees near Wrightwood, Science, 241, 196-199.

Jaeger, J., and N. Cook, 1979. Fundamentals of Rock Mechanics, 3rd ed., Chapman and Hall, London.

Johnson, K. M., and P. Segall, 2004. Viscoelastic earthquake cycle models with deep stress-driven creep along the San Andreas fault system, *J. Geophys. Res., 110*, B05S14, doi:10.1029/2004JB003096.

Kagan, Y. Y., D. D. Jackson, and Z. Liu, 2005. Stress and earthquakes in southern California, 1850-2004, *J. Geophys. Res., 110*, B05S14, doi:10.1029/2004JB003313.

Kagan, Y. Y., D. D. Jackson, and Y. F. Rong, 2006. A new catalog of southern California earthquakes, 1800-2005, Seismological Research Letters, 77(1), 30-38.

Kenner, S. J., and P. Segall, 1999. Time dependence of stress shadowing effect and its relation to structure of the lower crust*, Geology, 27*, 119-122.

Kenner, S. J., and P. Segall, 2003. Lower crustal structure in northern California: Implications from strain rate variations following the 1906 San Francisco earthquake, *J. Geophys. Res., 108*, 10.1029/2001JB000189.

Kenner, S. J., and M. Simons, 2005. Temporal clustering of major earthquakes along individual faults due to post-seismic reloading, *Geophys. J. Inter., 160*, 179-194.

Kilb D., J. Gomberg, and P. Bodin, 2000. Triggering of earthquake aftershocks by dynamic stresses, *Nature*, 408, 570-574.

King, G., R. Stein, and J. Lin, 1994. Static stress changes and triggering of earthquakes, *Bull. Seism. Soc. Am.*, 84, 935-953.

King, G. C. P. and M. Cocco, 2001. Fault interactions by elastic stress changes: new clues from earthquake sequences, *Adv. Geophys. 44*, 1-38.

Lin, J. and R. S. Stein, 2004. Stress triggering in thrust and subduction earthquakes and stress interaction between the southern San Andreas and nearby thrust and strike-slip faults, J. Geophys. Res., 109, doi:10.1029/2003JB002607.

Marsan, D., and C. J. Bean, 2003. Seismicity response to stress perturbations, analyzed for a world-wide catalogue, *Geophys. J. Inter., 154*, 179-195.

Meade, B. J., and B. H. Hager, 2005. Block models of crustal motion in southern California constrained by GPS measurements, J. Geophys. Res., 110, doi:10.1029/2004JB003209.

Nalbant, S., A. Hubert, and G. King, 1998. Stress coupling between earthquakes in northwest Turkey and the north Aegean sea, J. Geophys. Res., 103, 24,469-24,486.

Nostro, C., M. Cocco, and M. Belardinelli, 1997. Static stress changes in extensional regimes: an application to southern Apennines (Italy), *Bull. Seism. Soc. Am.*, 87, 234-248.

Parsons, T., R. Stein, R. Simpson, and P. Reasenberg, 1999. Stress sensitivity of fault seismicity: A comparison between limited-offset oblique and major strike-slip faults, *J. Geophys. Res.,* 104, 20,183-202.

Parsons, T., S. Toda, R. S. Stein, A. Barka, and J. H. Dietrich, 2000. Heightened odds of large earthquakes near Istanbul: An interaction-based probability calculation, Science, 288, 661-665.

Parsons T., 2002. Post-1906 stress recovery of the San Andreas fault system calculated from three-dimensional finite element analysis, J. Geophys. Res., 107, doi:10.1029/2001JB001051.

Parsons, T., 2006. Tectonic stressing California modeled from GPS observations, *J. Geophys. Res., 111*, doi:10.1029/2005JB003946.

Pollitz, F. F., and I. S. Sacks, 1992. Modeling of postseismic relaxation following the great 1857 earthquake, southern California, *Bull. Seism. Soc. Am.*, 82, 454-480.

Pollitz F., 1995. Consequences of stress changes following the 1891 Nobi earthquake, Japan. *Bull. Seism. Soc. Am.* 85, 796-807.

Pollitz, F., 1996. Coseismic deformation from earthquake faulting on a layered spherical earth, *Geophys. J. Int.,* 125, 1-14.

Pollitz, F., 1997. Gravitational-viscoelastic postseismic relaxation on a layered spherical earth. *J. Geophys. Res.* 102, 17921-17941.

Pollitz, F. F., G. Peltzer, and R. Bürgmann, 2000. Mobility of continental mantle; Evidence from postseismic geodetic observations following the 1992 Landers earthquake, *J. Geophys. Res., 105*, 8035-8054.

Pollitz, F., and I. Sacks, 2002. Stress triggering of the 1999 Hector Mine earthquake by transient deformation following the 1992 Landers earthquake, *Bull. Seism. Soc. Am.*, 87, 1-10.

Pollitz, F. F., 2003. Transient rheology of the uppermost mantle beneath the Mojave Desert, California, *Earth Planet. Sci. Lett., 215*, 89-104.

Pollitz, F. F., M. Vergnolle, and E. Calais, 2003. Fault interaction and stress triggering of 20th century earthquakes in Mongolia, *J. Geophys. Res., 108,* doi:10.1029/2002JB002375.

Pollitz, F. F. and M. Nyst, 2005. A physical model for strain accumulation in the San Francisco Bat Region, Geophys. J. Int, 160, 302-317.

Reasenberg, P., and R. Simpson, 1992. Response of regional seismicity to the static stress change produced by the Loma Prieta earthquake, *Science*, 255, 1687-90.

Rockwell T. K., S. Lindvall, M. Herzberg, D. Murbach, T. Dawson, G. Berger, 2000. Paleoseismology of the Johnson Valley, Kickapoo, and Homestead Valley faults: Clustering of earthquakes in the eastern California shear zone, *Bull. Seismol. Soc. Am., 90*, 1200-1236.

Rydelek, P., and I. Sacks, 2001. Migration of large earthquakes along the san Jacinto fault; stress diffusion from the 1857 Fort Tejon earthquake, *Geophys. Res. Lett.*, 28, 3079-3082.

Savage J. C., and M. Lisowski, 1998. Viscoelastic coupling model of the San Andreas fault along the Big Bend, southern California, *J. Geophys. Res., 103*, 7281-7292.

Scholz, C. H., 1988. Mechanics of seismic quiescences, *Pure Appl. Geophys., 126*, 701-718.

Scholz, C., 2002. The Mechanics of Earthquakes and Faulting, 2nd ed., Cambridge Univ. Press, New York.

Segall, P., 2002. Integrating geologic and geodetic estimates of slip rate on the San Andreas fault system, Inter. Geo. Rev., 44, 62-82.

Shearer, P. M., 1997. Improving local earthquake locations using the L1 norm and waveform cross correlation: Application to the Whittier Narrows, California, aftershock sequence, J. Geophys. Res., 102, 8269–8283.

Shen, Z.-K., et al., 2003. Southern California Earthquake Center Crustal Motion Map Version 3.0, http://epicenter.usc.edu/cmm3/, University of Southern California, Los Angeles, California.

Shewchuk, J. R., 1996, Triangle: Engineering a 2D Quality Mesh Generator and Delaunay Triangulator, First Workshop on Applied Computational Geometry (Philadelphia, PA), 124-133.

Sieh, K.E., M. Stuiver, and D. Brillinger, 1989. A more precise chronology of earthquakes produced by the San Andreas fault in southern California, *J. Geophys. Res.,* 94, 603–623.

Smith, B., and D. T. Sandwell, 2003. Coulomb stress accumulation along the San Andreas Fault system, J. Geophys. Res., 108(B6), 2296, doi:10.1029/2002JB002136.

Smith B. R., and D. T. Sandwell, 2006. A model of the earthquake cycle along the San Andreas Fault system for the past 1000 years, J. Geophys. Res., 111, doi:10.1029/2005JB003703.

Stein, R. S. and M. Lisowski, 1983. The 1979 Homestead Valley earthquake sequence, California: control of aftershocks and postseismic deformation, *J. Geophys. Res., 88*, 6477-6490.

Stein R. S., G. C. P. King, and J. Lin, 1992. Change in failure stress on the southern San Andreas fault system caused by the 1992 magnitude = 7.4 Landers earthquake, *Science, 258*, 1328-1332.

Stein, R., G. King, and J. Lin, 1994. Stress triggering of the 1994 M_w=6.7 Northridge, California earthquake by its predecessors, *Science*, 265, 1432-1435.

Stein, R. S., 1999. The role of stress transfer in earthquake occurrence. *Nature, 402*, 605-609.

Stein, R. S., 2003. Earthquake conversations, *Sci. Amer., 288*, 72-79.

Thatcher, W., 1983. Nonlinear strain buildup and the earthquake cycle on the San Andreas fault, *J. Geophys. Res*., 88, 5893-902..

Toda, S., R. Stein, P. Reasonberg, J. Dieterich, and A. Yoshida, 1998. Stress transferred by the 1995 M_w=6.9 Kobe, Japan, shock: Effect on aftershocks and future earthquake probabilities, *J. Geophys. Res.,* 103, 24,543-65.

Toda, S., and R. S. Stein, 2002. Response of the San Andreas fault to the 1983 Coalinga-Nuñez earthquakes: An application of interaction-based probabilities for Parkfield, J. Geophys. Res., 107(B6), 2126, doi:10.1029/2001JB000172.

Toda, S., and R. Stein, 2003. Toggling of seismicity by the 1997 Kagoshima earthquake couplet: A demonstration of time-dependent stress transfer, J. Geophys. Res., 108(B12), 2567, doi:10.1029/2003JB002527.

Toda, S., R. S. Stein, K. Richards-Dinger, and S. B. Bozkurt, 2005. Forecasting the evolution of seismicity in southern California: Animations built on earthquake stress transfer, J. Geophys. Res., 110, B05S16, doi:10.1029/2004JB003415.

Turcotte, D. L. and G. Schubert, 2002. Geodynamics, 2nd edition, Cambridge University Press, pp. 456.

Wdowinski, S., Y. Sudman, and Y. Bock, 2001. Geodetic detection of active faults in southern California, *Geophysical Research Letters*, 28, 2321-2324.

Wyss, M., and S. Wiemer, 2000. Change in the probability for earthquakes in southern California due to the Landers magnitude 7.3 earthquake, *Science*, 290, 1334-1338.

Zeng Y., 2001. Viscoelastic stress-triggering of the 1999 Hector Mine earthquake by the 1992 Landers earthquake, *Geophys. Res. Lett., 28*, 307-3010.

Zoback, M. D., et al., 1987. New evidence on the state of stress of the San Andreas fault system, Science, 238, 1105 – 1111.